Electronic Supplementary Information

Antimony-doped $Bi_{0.5}Sr_{0.5}FeO_{3-\delta}$ as a novel Fe-based oxygen reduction electrocatalyst for solid oxide fuel cells below 600 °C

Lei Gao,[a] Qiang Li,*[a] Liping Sun,[a] TianXia,[a] Lihua Huo,[a] Hui Zhao*[a] and Jean-Claude Grenier[b]

[a]*Key Laboratory of Functional Inorganic Material Chemistry, Ministry of Education, School of Chemistry and Materials Science, Heilongjiang University, Harbin 150080 P. R. China.*

[b]*CNRS, Université de Bordeaux, ICMCB, 87 avenue du Dr. A. Schweitzer, F-33608 Pessac-Cedex, France*

** Corresponding author: E-mail address: liqiang@hlju.edu.cn (Q. Li)*

** Corresponding author: E-mail address: zhaohui98@yahoo.com (H. Zhao)*

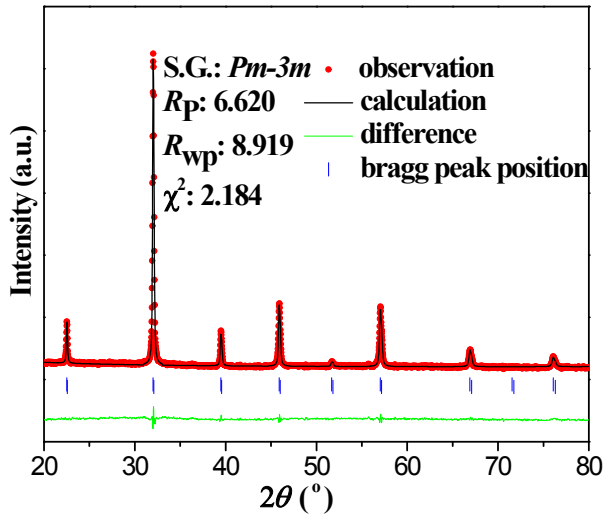

Fig. S1. XRD patterns and Rietveld refinement of the BSFS. Observed (red circles), calculated by the Rietveld method (black line), difference (green line), and calculated Bragg positions (blue vertical bar) for each phase are presented.

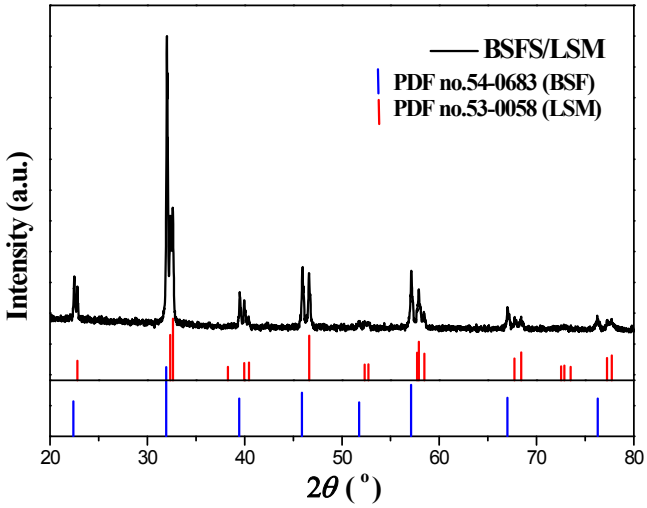

Fig. S2. XRD patterns of the BSFS/LSM composite powders after calcined at 1000 °C. The samples show a set of peaks that are well indexed to the cubic BSF phase (PDF-2 card no. 54-0683) and rhombohedral phase LSM (PDF-2 card no. 53-0058).

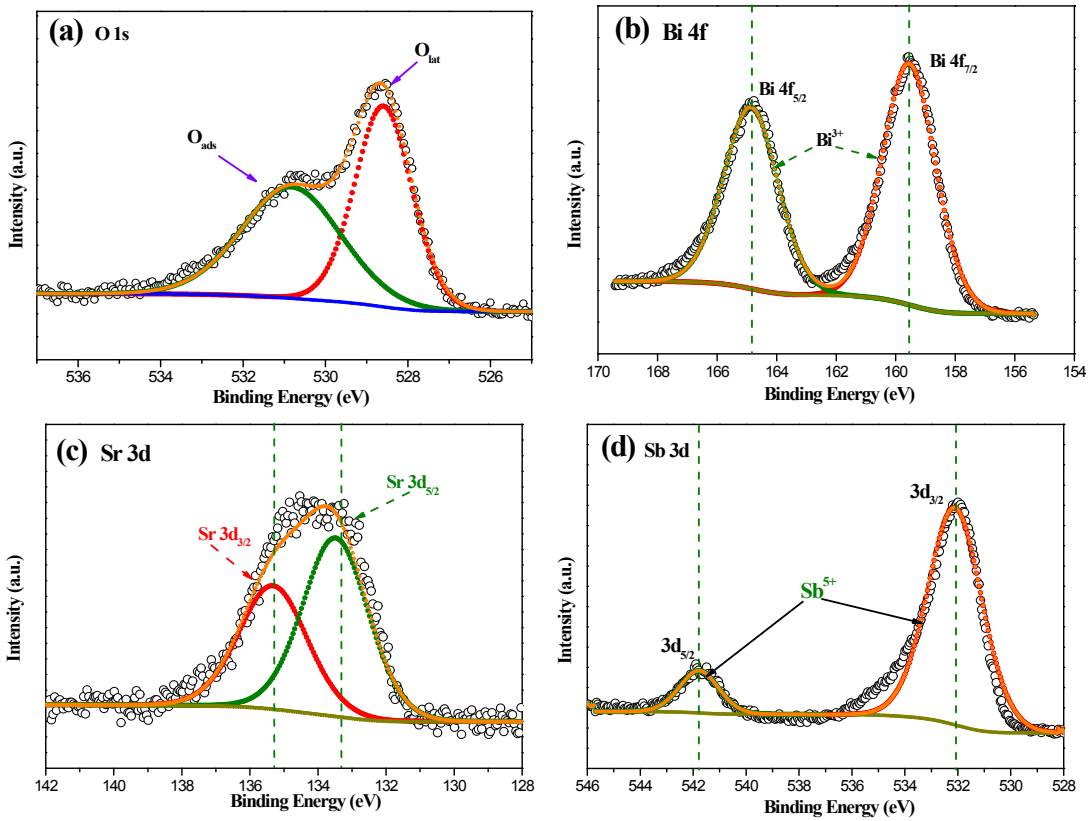

Fig. S3. XPS spectra fitting of (a) O 1s of BSF, (b) Bi 4f, (c) Sr 3d and (d) Sb 3d of BSFS.

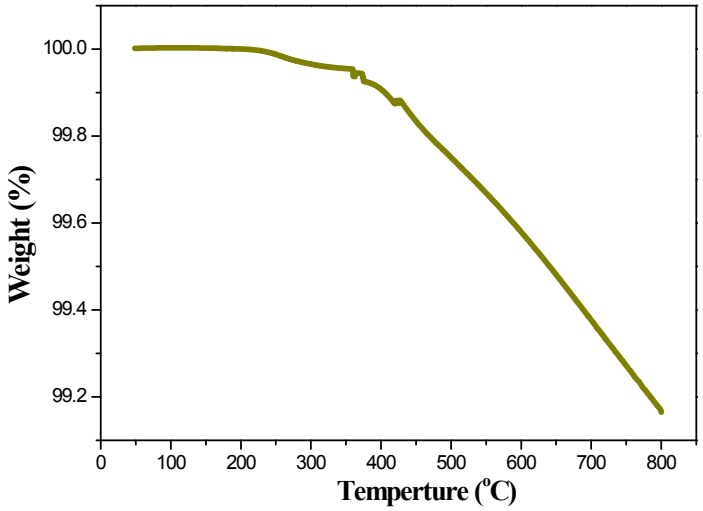

Fig. S4. Thermogravimetric data of BSFS was measured between 50 and 800 °C.

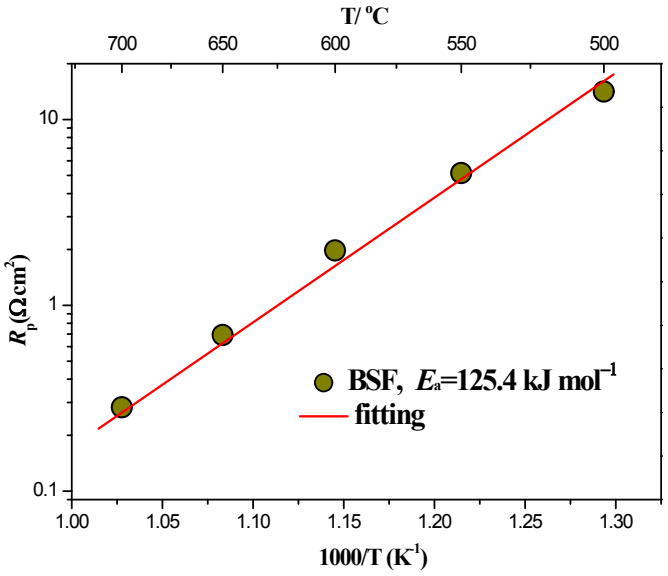

Fig. S5. Arrhenius plots of R_p for BSF cathode.

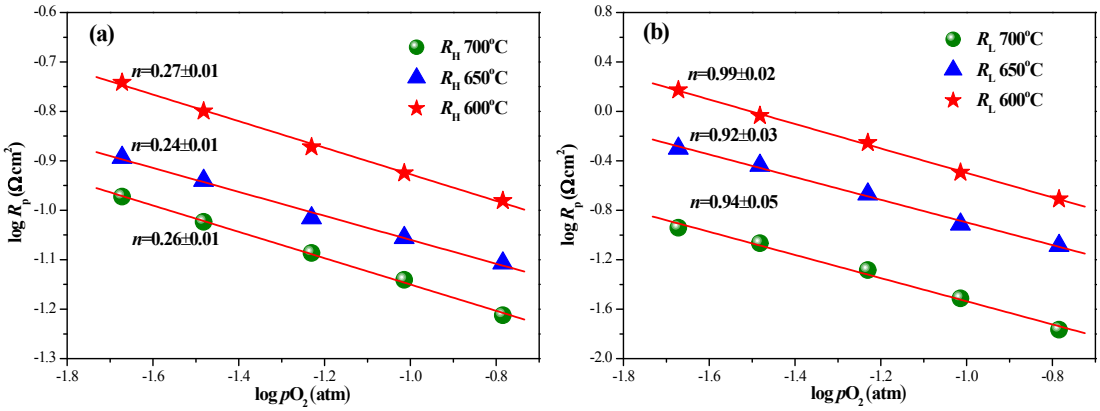

Fig. S6. Dependences of (a) R_{HF} and (b) R_{LF} of BSFS electrode on oxygen partial pressure at 600–700 °C.

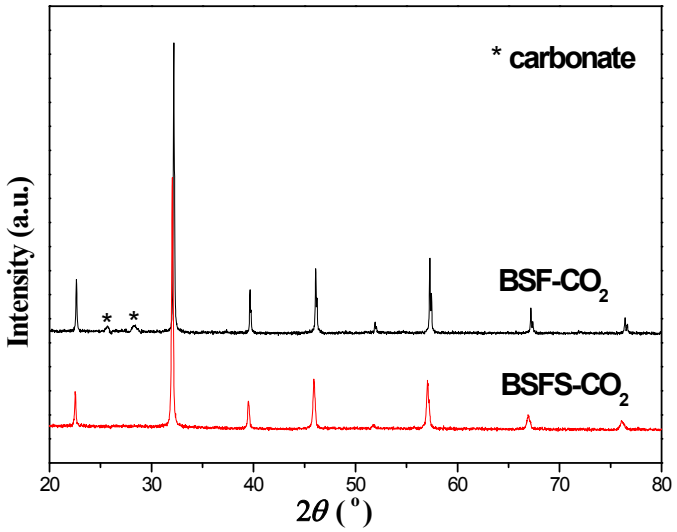

Fig. S7. Powder x-ray diffraction patterns of (a) BSF and (b) BSFS samples after 10 vol.% CO_2 exposure for 24 h at 800 °C.

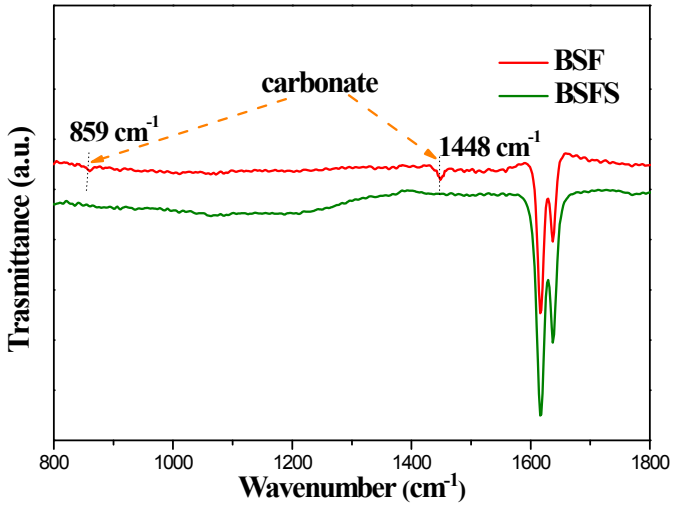

Fig. S8. FT-IR spectra of the (a) BSF and (b) BSFS samples treated under CO_2 at 800 °C for 24 h. The orange arrows indicate the vibrational peaks of CO_3^{2-}.

Table S1 Ratio of O_{ads}/O_{lat}, average valence of Fe and oxygen non-stoichiometry are calculated by XPS and iodometric titration (IT) at RT.

Sample	Type	O_{ads}/O_{lat}	Average (Fe)	δ
BSFS	XPS	2.51	2.88	0.204
	IT	–	2.91	0.191

Table S2 Oxygen nonstoichiometry (δ) value of different cathode materials at 600 °C.

Cathode materials	BSFS	SCS	SSCN	SFN
δ (600 °C)	0.33	0.29	0.12	0.30
Ref.	this work	S1	S2	S3

BSFS: $Bi_{0.5}Sr_{0.5}Fe_{0.9}Sb_{0.1}O_{3-\delta}$, SCS: $SrCo_{0.9}Sb_{0.1}O_{3-\delta}$, SSCN: $Sm_{0.5}Sr_{0.5}Co_{0.9}Nb_{0.1}O_{3-\delta}$, SFN: $SrFe_{0.9}Nb_{0.1}O_{3-\delta}$

Table S3 Comparison of R_P and peak power density of BSFS cathode with some other reported cathodes in the literatures at 600 °C.

Cathode	Anode-supported Electrolyte	R_P (Ω cm^2) 600 °C	Peak power Density (W cm^{-2})	Ref.
$Bi_{0.5}Sr_{0.5}Fe_{0.90}Sb_{0.10}O_{3-\delta}$	YSZ+NiO YSZ	0.098	0.94	this work
$SrFe_{0.85}Ti_{0.1}Ni_{0.05}O_{3-\delta}$	YSZ+NiO YSZ	0.15	0.68	S4
$Bi_{0.5}Sr_{0.5}Fe_{0.90}Nb_{0.10}O_{3-\delta}$	YSZ+NiO YSZ	0.17	0.71	S5
$La_{0.6}Sr_{0.4}Co_{0.2}Fe_{0.8}O_{3-\delta}$	YSZ+NiO YSZ	3.53	0.12	S6
$Gd_{0.6}Sr_{0.4}Fe_{0.8}Co_{0.2}O_{3-\delta}$	CGO+NiO CGO	0.89	0.49	S7
$BaFe_{0.95}Sn_{0.05}O_{3-\delta}$	YSZ+NiO YSZ	0.21	0.39	S8
$Pr_{0.5}Sr_{0.5}$ $Fe_{0.8}Cu_{0.2}O_{3-\delta}$	YSZ+NiO YSZ	0.34	0.24	S9
$Bi_{0.5}Sr_{0.5}Fe_{0.80}Co_{0.20}O_{3-\delta}$	SDC+NiO SDC	0.38	0.31	S10
$Ba_{0.5}Sr_{0.5}Fe_{0.8}Cu_{0.2}O_{3-\delta}$	SDC+NiO SDC	0.36	0.31	S11
$La_{0.6}Sr_{0.4}Fe_{0.90}Mo_{0.10}O_{3-\delta}$	BZCY+NiO BZCY	0.58	0.23	S12

References:

S1 A. Aguadero, M. Retuerto, F. Jiménez-Villacorta, M. T. Fernandez-Diaz and J. A. Alonso, *Phys. Chem. Chem. Phys.*, 2011, **13**, 12835–12843.

S2 S. Yoo, T. Lim and G. Kim, *J. Power Sources*, 2013, **226**, 1–7.

S3 S. S. Jiang, J. Sunarso, W. Zhou, J. Shen, R. Ran and Z. P. Shao, *J. Power Sources*, 2015, **298**, 209–216.

S4 G. Yang, W. Zhou, M. Liu and Z. Shao, *ACS Appl. Mater. Interfaces*, 2016, **8**, 35308–35314.

S5 L. Gao, Q. Li, L. P. Sun, X. F. Zhang, L. H. Huo, H. Zhao and J. C. Grenier, *J. Power Sources*, 2017, **371**, 86–95.

S6L. E. Wu, L. Zhao, Z. L. Zhan and C. R. Xia, *J.Power Sources,* 2014, **266**, 268–274.

S7 K. K. Hansen, K. V. Hansen and M. Mogensen, *J. Solid State Electrochem.*, 2010, **14**, 2107–2112.

S8 F. F. Dong, M. Ni, W. He, Y. B. Chen, G. M. Yang, D. J. Chen and Z. P. Shao, *J. Power Sources*, 2016, **326**, 459–465.

S9 J. Lu, Y. M. Yin, J. Yin, J. Li, J. Zhao and Z. F. Ma, *J. Electrochem. Soc.*, 2016, **163** F44–F53.

S10 S. G. Huang, F. Gao, Z. Meng, S. J. Feng, X. H. Sun, Y. D. Li and C. C. Wang, *Chemelectrochem*, 2014, **1**, 554–558.

S11 L. Zhao, B. B. He, X. Z. Zhang, R. R. Peng, G. Y. Meng and X. Q. Liu, *J. Power Sources*, 2010, **195**, 1859–1861.

S12 T. Xu, X. B. Mao and G. L. Ma. Meng, *Ceram. Int.*, 2014, **40**, 13747–13751.